ELSEVIER

Journal of Membrane Science 164 (2000) 111–120

journal of MEMBRANE SCIENCE

www.elsevier.nl/locate/memsci

Effect of solvent evaporation on the formation of asymmetric and symmetric membranes with crystallizable EVAL polymer

Tai-Horng Young *, Yao-Huei Huang, Li-Yen Chen

Institute of Biomedical Engineering, College of Medicine and College of Engineering, National Taiwan University, Taipei 10016, Taiwan

Received 7 December 1998; received in revised form 29 March 1999; accepted 20 May 1999

Abstract

The effect of the evaporation process on the nonsolvent-induced phase inversion in the poly (ethylene-co-vinyl alcohol) (EVAL)/DMSO/water system was investigated. The duration of the evaporation process correlated with the resultant membrane morphologies via scanning electron microscope. Surprisingly, evaporation time not only played an important role in the existence of macrovoids, but also affected membrane morphology from sponge structure to particulate structure. Macrovoids were found within a membrane if the casting was immediately immersed into water bath or the evaporation time was less than 15 min, while macrovoids diminished and sponge structure appeared with evaporation time of 30 min. When the evaporation time was 45 and 60 min, a symmetric membrane consisting of a packed bed of nearly equal-diameter particles dominated by the solid–liquid demixing process was observed. This suggests that crystallization of EVAL polymer from the evaporated solution inhibited the formation of an asymmetric membrane with cellular pores dominated by the liquid–liquid demixing process. Compared with the corresponding phase diagram, such a crystallization process depends on how deep the solid–liquid demixing region is entered. The results of this study show that the structure of membranes can be well controlled by the knowledge of membrane formation mechanism.

Keywords: Evaporation; Membrane morphology; Crystallization; Liquid–liquid demixing

1. Introduction

The technological importance of polymer membranes in the separation industries is well-documented [1]. Most commercial membrane production is based on the nonsolvent-induced phase inversion process [2]. For a given polymer system, the membrane structure determines the separation characteristics. The basic principle of controlling membrane structures from a crystallizable polymer is the competition between the liquid–liquid demixing process and the solid–liquid demixing process. Liquid–liquid demixing results in the typical cellular morphology. Solid–liquid demixing originated from crystallization of regular segments of polymer brings particulate feature to the morphology of the membrane [3–9]. In our laboratory, we have prepared poly (ethylene-co-vinyl alcohol) (EVAL) membranes with particulate morphology characterized by a packed bed of nearly equal-diameter particles approximately in the submicron order [8–10]. Such particulate membranes have proved useful in

* Corresponding author. Tel.: +886-2-2397-0800/1455; fax: +886-2-2394-0049.
E-mail address: thyoung@ha.mc.ntu.edu.tw (T.-H. Young).

0376-7388/00/$ – see front matter
PII: S0376-7388(99)00210-0

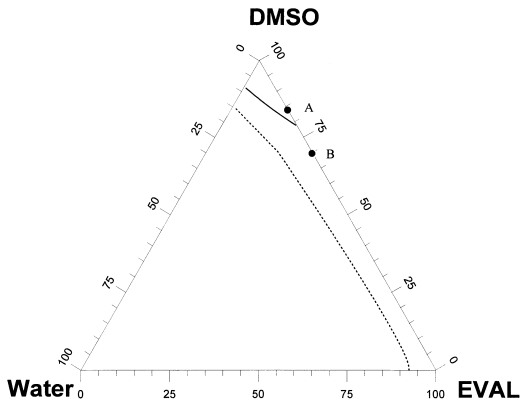

Fig. 1. Phase diagram of water-DMSO–EVAL at 25°C [8]. (▬▬: crystallization equilibrium line;– – –: binodal boundary).

plasma protein separation [11] and microfiltration [12].

The competition between liquid–liquid demixing and solid–liquid demixing can be understood through the corresponding thermodynamic (phase behavior) and kinetic (mass transfer) aspects of the immersion-precipitation process [9,13–15]. The phase diagram of the ternary system, water-DMSO-EVAL at 25°C has been described previously [8]. As shown in Fig. 1, there is a one-phase region and two two-phase (solid–liquid demixing and liquid–liquid demixing.) regions lying within the triangle. The liquid–liquid demixing boundary (i.e., binodal) is located inside the solid–liquid demixing region. Therefore, if a casting solution has the composition on the solvent/ polymer axis of the one-phase region as indicated in point A, the casting solution, after immersing in the precipitation bath, will enter the solid–liquid demixing region prior to the liquid–liquid demixing region. However, apart from thermodynamics also kinetics will play an important role in the membrane formation. Liquid–liquid demixing usually proceeds very rapidly. While polymer crystallization always proceeds at a certain degree of undercooling and is thus strongly dependent on the solvent/nonsolvent exchange rate. Hence, if the mass transfer is very rapid, it is possible that solid–liquid demixing is overlooked and the casting solution may remain homogeneous until the binodal is entered. Consequently, liquid–liquid demixing may take place first to dominate the membrane structure. On the other hand, if the mass transfer is not rapid, the polymer has the opportunity to become supersaturated with respect to crystallization and crystallization nucleation is probably to occur during membrane formation.

Overall, the time that is available for the membrane solution within the solid–liquid demixing region before it enters the liquid–liquid demixing region is important to determine which type of phase separation will take place. For example, when two systems have the same diffusion kinetics, the system with larger distance in location of the equilibrium crystallization line and the binodal will have more time for polymer to crystallize. Conversely, when two systems have the same phase behavior, the system with slower diffusion kinetics distance will have more time for polymer to crystallize. The introduction of an evaporation process has the same effect in increasing the time of the membrane solution within the solid–liquid demixing region. After elimination of the solvent, the sample A in Fig. 1 can move to B situated between the equilibrium crystallization line and the binodal boundary. Since this supersaturated solution has remained for a long time, it has the opportunity for polymer to crystallize. Therefore, the purpose of this paper is to examine whether crystal nuclei induced by an evaporation process may result in a change of the membrane structure in the subsequent immersion into a nonsolvent bath. Experiments were carried out to investigate EVAL membrane morphologies as a function of the period of evaporation. Although there are several models proposed to describe the solvent evaporation pertinent to the membrane formation [16–19], the validity of these model is only restricted to the amorphous polymer membrane. These theories are not satisfactory in explaining the formation of membranes from crystallizable polymers. In addition, in a previous article, we have investigated the effect of the very short (5 min) and very long (1 day) period of the evaporation process on the membrane structure from a supersaturated polymer solution [20]. However, that study did not clearly analyze the influence of crystallization on the different membrane structures due to the change of the duration of the evaporation process. This present study therefore, provides us to fundamentally understand the effect of the evaporation process on the formation of asymmetric and symmetric membranes with crystallizable EVAL polymer.

2. Experimenatal

2.1. Membrane preparation

Membranes were prepared by using EVAL (105A, Kuraray, Japan) having an average ethylene content of 44 mole%. DMSO of extra pure reagent grade (Nacalai Tesque, Kyoto, Japan) was used as the solvent for EVAL. The nonsolvent for EVAL was deionized and double-distilled water.

EVAL membranes were prepared from a 15 wt.% of EVAL solution. This solution was dispersed uniformly on a glass plate (ca. 100 μm) by an autocoater (KCC303, RK Print-Coat Instruments, UK). Since the evaporation rate of DMSO is very low, the casting solution was evaporated in a vacuum oven at 6 cm Hg. Before and after a period of evaporation time (0–60 min), the weights of the plate plus the casting solution were recorded to evaluate the composition change of the casting solution. The evaporated solution was then immersed into a water bath where it remained until the membrane was completely formed. All the process was performed at 25°C. These prepared membranes were examined on freeze-dried samples to observe the transition from finger-to sponge and sponge-to particulate morphologies using a scanning electron microscope (SEM).

2.2. Light transmission experiment

Light transmission experiments were performed to measure the time of the appearance of optical inhomogenities of the casting solution in the water bath. The principle is that the light transmittance would decrease due to the optical inhomogenities, which can be induced by liquid–liquid demixing or solid–liquid demixing. Therefore, the time that the light transmittance begins to drop can be used to represent the time of the onset of phase separation of the casting solution in the water bath. To carry out the light transmission experiment, a lamp was placed above the precipitation bath as light source and a light detector beneath the water bath was used to measure the light transmittance. For detailed experimental setup and procedures, one can refer to the work of Reuvers et al [13]. In addition, to investigate the possible effect of the evaporation process on the appearance of optical inhomogenities in the evaporated solution light transmittance experiments were performed prior to and behind the evaporation process. No differences could be detected.

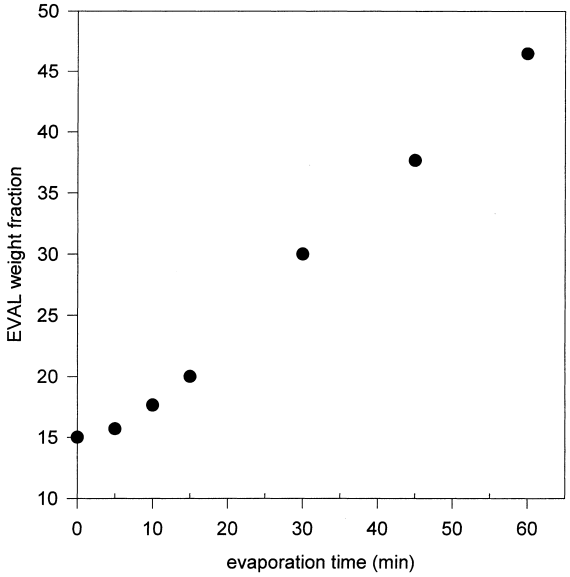

Fig. 2. EVAL weight fraction of a 15 wt.% EVAL solution after various solvent evaporation times.

3. Results

3.1. Solvent evaporation

Fig. 2 shows the weight fraction of EVAL due to DMSO loss as a function of evaporation time. The data were determined gravimetrically by measuring the weight change of the evaporated solution. It should be pointed out that concentration gradients would be present within the casting solution during evaporation [21]. For simplicity, it is assumed that a flat concentration profile is within the casting solution when the low volatility of DMSO leaving from the surface of the casting solution can be compensated by DMSO diffusion from the casting solution interior to the surface. This assumption will be further examined and rationalized in Section 4.

3.2. Light transmission

In Fig. 3, light transmittance profiles are shown for precipitation of a 15 wt.% EVAL solution in a

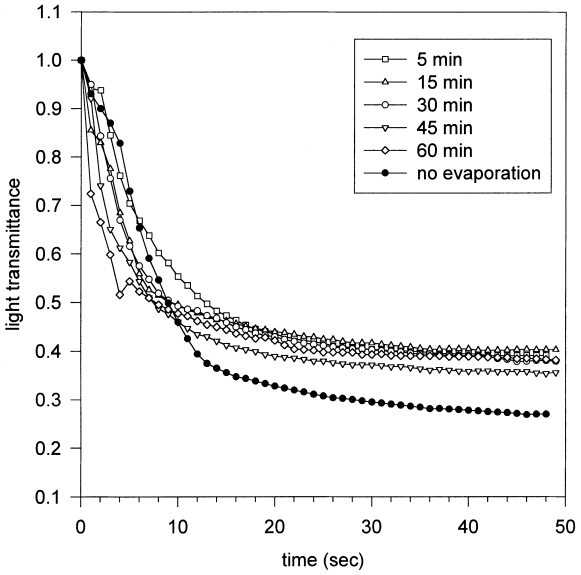

Fig. 3. Light transmittance profiles for precipitation of a 15 wt.% EVAL solution in a water bath after various solvent evaporation times.

water bath after various solvent evaporation times. It appears that all the light transmission intensity of the membrane solution decreased by about 50% after immersion for 10 s. Therefore, the instantaneous demixing took place in all membrane formation cases. Before immersing the evaporated solution into the water bath, the EVAL weight fraction is ranged from 0.15 to 0.47 (Fig. 2). This indicates that both the DMSO and water diffusivities in the water/DMSO/EVAL system can be taken as effectively constants in the range $0.15 < \text{EVAL concentration} < 0.47$ since the membrane formation dynamics is determined by the diffusion rates of solvent and nonsolvent.

3.3. Morphological studies

Representative SEM photographs associated with the membranes cast under various evaporation times are presented in Figs. 4–7. There are six sets of micrographs which cover the entire evaporation-time range studied here. In Fig. 4, morphologies of the membrane are shown for the direct immersion of casting solution into a water bath without the evaporation step. Fig. 4(a) shows the top surface of this membrane has a tight morphology. Fig. 4(b) shows the support layer contains large finger-like macrovoids extending almost to the bottom surface. In addition, the cross-section region near top surface at higher magnification shows a thin dense skin layer and cellular pores enclosed in a polymer matrix, similar to those of amorphous membranes are observed. Cellular structures are the evidence of liquid–liquid demixing mechanism. Therefore, the phase separation process dominating this membrane formation is liquid–liquid demixing. However, the binodal boundary is below the equilibrium crystallization line from the phase diagram of water-DMSO-EVAL at 25°C as shown in Fig. 1. One should expect crystallization-induced morphology will be present in the membrane because the composition path crosses the equilibrium crystallization line earlier than the binodal. But typical morphology characteristic of polymer crystallization (i.e., particulate, discussed previously [3–9]) is not observed within this membrane. This suggests that the induction time is not long enough for solid–liquid demixing to nucleate, which is consistent with the observed immediate turbidity in the light transmission measurement (Fig. 3). Hence, the membrane structure is contrary to the prediction on basis of the thermodynamic point of view.

When 5 min of evaporation time was employed, the membrane structure is identical to the membrane for the direct immersion of casting solution into a water bath without the evaporation step (not shown here). A dense skin layer is on the membrane surface and macrovoids extend into the sublayer. This suggests that the membrane formation mechanism in these two systems is similar. Therefore, the effect of increasing the polymer concentration by evaporating DMSO of the casting solution for 5 min on the membrane structure is not significant.

When 15 min of evaporation time was employed, the system still underwent liquid–liquid demixing resulting in an asymmetric morphology with prominent macrovoids (not shown here). The polymer concentration is roughly 20 wt.% for up to 15 min of evaporation time (Fig. 2). This implies the casting solution is still above the equilibrium crystallization line (Fig. 1). Therefore, it is reasonable that the mechanism of membrane formation mechanism in the above three membranes is the same.

Fig. 5 presents the top and cross-sectional views of the membrane prepared with evaporation time of 30 min. The top surface of this membrane forms a

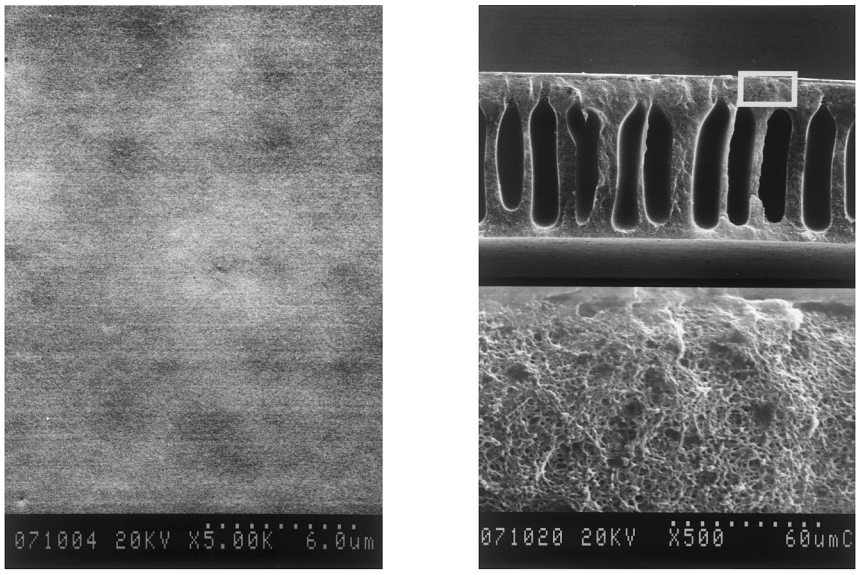

Fig. 4. SEM photomicrographs of membrane from a 15 wt.% of EVAL solution immersed in water without the evaporation step. (a) Top surface; (b) cross-section.

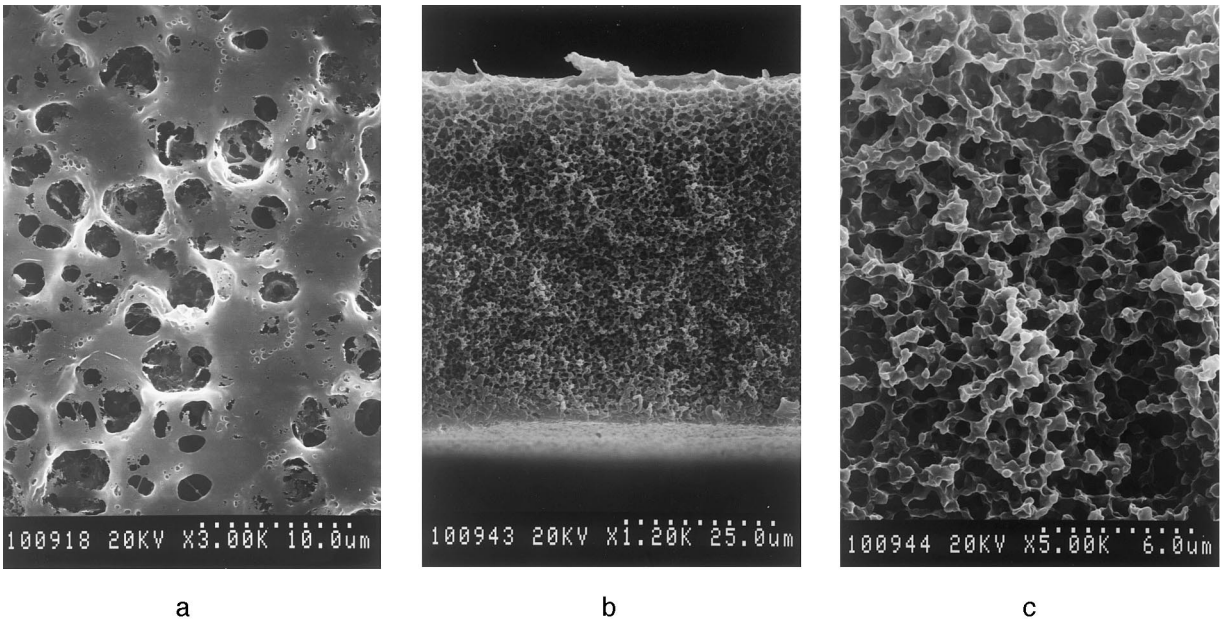

Fig. 5. SEM photomicrographs of membrane from a 15 wt.% of EVAL solution immersed in water after 30 min of evaporation. (a) Top surface; (b) cross-section; (c) magnification of (b).

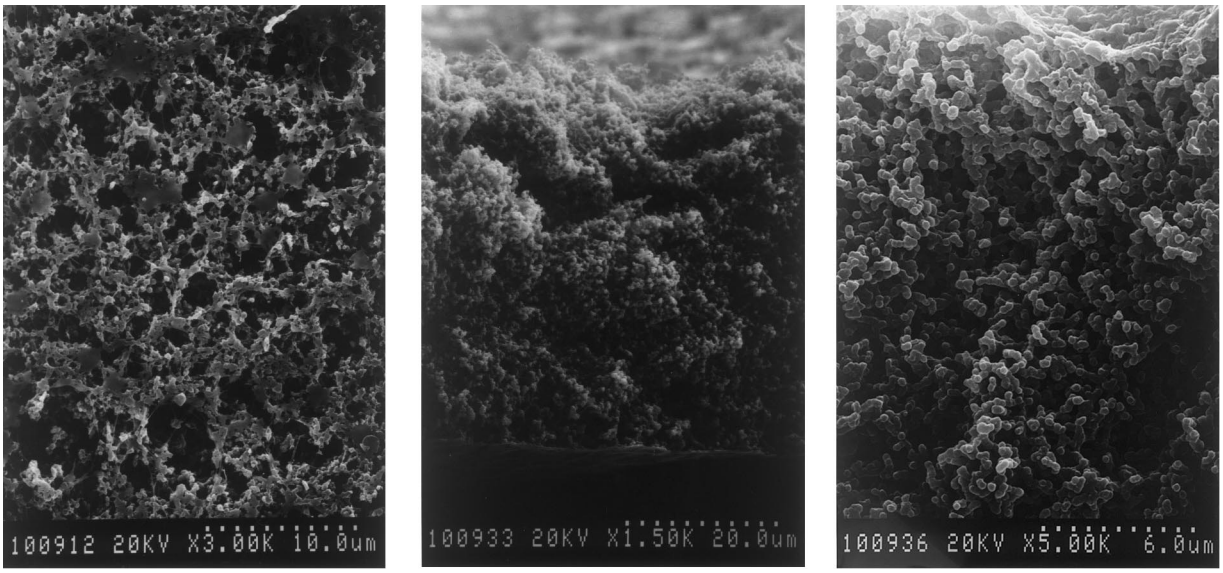

Fig. 6. SEM photomicrographs of membrane from a 15 wt.% of EVAL solution immersed in water after 45 min of evaporation. (a) Top surface; (b) cross-section; (c) magnification of (b).

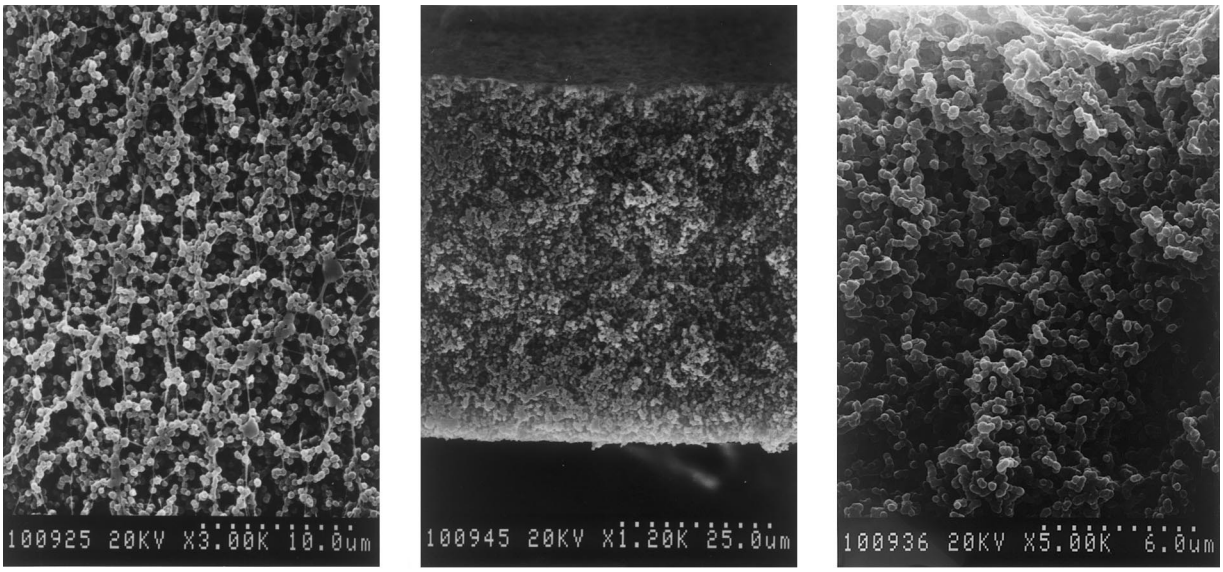

Fig. 7. SEM photomicrographs of membrane from a 15 wt.% of EVAL solution immersed in water after 60 min of evaporation. (a) Top surface; (b) cross-section; (c) magnification of (b).

microporous skin (Fig. 5(a)). Once the casting solution contacts nonsolvent, the top surface rapidly forms a high polymer concentration layer according to the liquid–liquid equilibrium with the precipitation bath [9,13]. Therefore, a microporous skin will be formed when the cellular nuclei are formed near the skin, which can grow through the skin [22]. The cross-section of this membrane represents the completely cellular structure (Fig. 5(b)). Although an instantaneous demixing can be seen in the light transmission experiment (Fig. 3), columnar fingers are no longer present. Mechanism for the formation of finger-like macrovoids is beyond the scope of the current work. However, a membrane formation system with an instantaneous liquid–liquid demixing mechanism generally favors macrovoid morphology [22]. The reason for the elimination of macrovoid in a membrane system with an instantaneous liquid–liquid demixing property may be due to that a greater viscosity of a more concentrated polymer solution at the point of precipitation prohibits the growth of macrovoids [23]. Therefore, increasing the polymer concentration by a longer evaporation time suggests an unfavorable condition for macrovoid membrane formation but favorable for sponge membrane formation.

Details of the cellular structure are shown at higher magnification in Fig. 5(c). The uniformity of the sponge structure suggests that it is dominated by the liquid–liquid demixing process. Furthermore, it is apparent that the cell walls formed by the polymer-rich phase are deformed and irregular. Almost all of the pore walls are open and interconnected to yield a bi-continuous structure. Such morphology may be caused partly by liquid–liquid demixing and partly by crystallization. As the polymer-rich wall after liquid–liquid demixing is always in a supersaturated state with respect to crystallization (see the phase diagram in Fig. 1), polymer can crystallize from the amorphous gel into the solid matrix [24]. This suggests that crystallization occurs at the late stage of precipitation and the cellular structure has largely been fixed. Hence, the membrane exhibits a cellular structure similar to that of an amorphous membrane. Crystallization leaves its imprint only on the cell walls.

When 45 min of evaporation time was employed, the structure of the membrane underwent dramatic changes. Unlike that observed in Fig. 4(a), this surface is porous and particles are formed in the top surface as shown in Fig. 6(a). This implies that precipitation of EVAL is not dictated by liquid–liquid demixing only and particle aggregate formation due to crystallization has become a competitive or even predominant phase separation mechanism for this membrane. The cross-section of this membrane, as shown in Fig. 6(b) and (c), is composed of globular particles that interlock to form a totally open bi-continuous network. Cellular pores resulted from liquid–liquid demixing process are not evident.

After 60 min of long evaporation period, the structure of the top surface is practically identical to the membrane bulk region as shown in Fig. 7. Unlike the membrane with somewhat flattened and dense structure shown in Fig. 6(a), the surface exhibits no dense region at all (Fig. 7(a)). As the structure of the membrane's cross-section resembles that of the top surface, this membrane is characterized by a symmetric and homogeneous morphology. At this time solid–liquid demixing in the membrane is undoubtedly occurring by a nucleation and growth mechanism. These nuclei then grow until their fronts impinge each other to form a particulate membrane. Therefore, no cellular morphology due to liquid–liquid demixing was found in this membrane.

4. Discussion

The membranes prepared in this work indicate that a wide range of morphologies can be associated with different evaporation periods during membrane formation. This difference clearly implies that they should have different diffusion kinetics when the formation of these membranes is in the same phase diagram. Especially, liquid–liquid demixing and crystallization occur on two different time scales so the possibility of crystallization can complicate the effect of evaporation on the crystalline polymer membrane. As usual, the composition path for a membrane prepared by a direct precipitation process follows the line 'a' in Fig. 8. Start at point "0", a mixture of polymer and solvent, it will cross the equilibrium crystallization line first and then the binodal due to the exchange of solvent and nonsolvent. In this circumstance, crystallization should happen first, but if the diffusion process

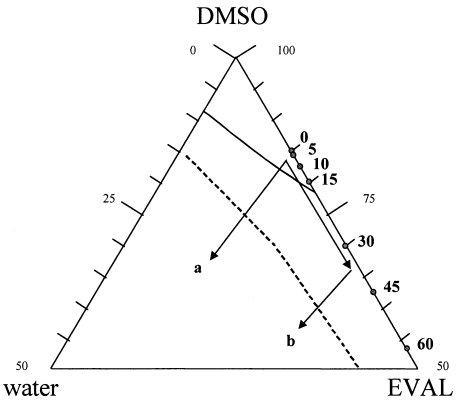

Fig. 8. Composition paths for precipitation of a 15 wt. % EVAL solution in a water bath (▬▬▬: crystallization equilibrium line; – – –: binodal boundary). (a) without evaporation; (b) with evaporation. The numbers shown denote evaporation time.

is very fast then the time for the membrane solution in the solid–liquid demixing region is too short to allow a crystallization process to occur. As a result, liquid–liquid demixing process dominates the membrane formation mechanism and an asymmetric membrane with cellular pores is formed.

As described above, when there is enough time to undergo solid–liquid demixing, it is expected that crystallization will occur. Based on this concept, the composition path will follow the line 'b1' corresponding to Fig. 8 and will not pass the binodal at all when DMSO leaves the casting solution by evaporation instead of the exchange of solvent and nonsolvent by diffusion. Thus, crystallization has more time to develop. The data points with different times in Fig. 8, which correspond to the composition of the evaporated solution in Fig. 2, indicate that the composition is above the equilibrium crystallization line in the shorter evaporation time. About 15 min of DMSO evaporation is needed for the composition path to arrive at the solid–liquid demixing region. Therefore, when the evaporation time is less than 15 min, the evaporated solution is still a good solution in which polymer chain is well solvated. Of course, the effect of 15 min of evaporation on the membrane structure is not significant. By contrast, when the evaporation time is increased, the evaporated solution, such as 45 and 60 min of evaporation time, is in a metastable state with respect to crystallization wherein the originally extended coil will associate into an aggregated structure. Such a solution contains a large population of subcritical crystal embryos. As a result, the evaporation process enhances the capability of the system to crystallize and particular membranes can be produced in this way; see Figs. 6 and 7. However, it seems a composition just below the equilibrium crystallization line can not form nuclei. Such a case is observed as 30 min of evaporation time was employed. Although the composition of the evaporated solution (30 wt.% EVAL in DMSO) is situated in the solid–liquid demixing region, crystallization and liquid–liquid demixing separation almost begin at a close time frame; see Fig. 5. This can be attributed to the fact that the nucleation and growth rates of the crystals increase by increasing the degree of polymer supersaturation. In order to precisely describe the evaporation time that govern particulate membrane development, it is of interest to express the crystallization temperature for 30 wt.% EVAL solution is about 45°C; see Fig. 2 in our previous report [8]. Therefore, the supercooling temperature is 20°C for this case. This result illustrates that a large degree of supersaturation is necessary for crystallization process to dominate the resulting membrane structure.

Compared with the membranes prepared from 0–60 min of evaporation time, it can be deduced that the structure of membranes is depended on which phase inversion is happened. Moreover, the sequence of crystallization and liquid–liquid demixing depends on the supersaturation degree of the solution. Therefore, it suggests that the evaporation step increases the ability of EVAL to crystallize by increasing polymer concentration to enhance the driving force for crystal nucleation.

Although the nuclei of particles are initiated in the stage of evaporation, the growth of nuclei may be hindered by the limitations in polymer diffusion in the high entanglement condition. Therefore, no differences in the light transmission of a polymer solution before and after evaporation could be detected because the diameter of nuclei is small compared with the wavelength of the light. After evaporation, the composition path will follow the line 'b2' corresponding to Fig. 8 by immersing the evaporated solution into water; at which time, binodal miscibility boundary is entered. This indicates that liquid–liquid demixing process is responsible for the growth of a particle in the

subsequent immersion into a water bath. This growth stops when its advancing front meets other particles. That is to say the particulate morphology is attributed to a cascade of phase transitions. First, solid–liquid demixing induces the formation of particle nuclei. Second, due to liquid–liquid demixing the particle growth is induced in the medium surrounding the particle nuclei. Therefore, regardless of the evaporation time, the entire demixing rate from the light transmission experiments are instantaneous (Fig. 3). However, at this time, the liquid–liquid demixing only plays a minor role in determining the membrane structure because the formation of nuclei in the evaporation process has determined the characteristics of the resulting membrane structure.

Last, a composition path describes the place and time-dependent composition of the polymer solution. However, the gravimetric method used to measure the composition change of the casting solution during the evaporation process allows only determination of an average composition. Therefore, data of Fig. 2 allowed us to draw average composition paths in the triangular phase diagram as shown in Fig. 8 when concentration gradient may be neglected during the evaporation process. In this work, crystallization far below the equilibrium crystallization line forms many nuclei, and particles grow until their fronts impinge each other. Since the particle size requires the determination of the induction time before any developing nuclei appear, particles in Fig. 7 having a uniform size is an evidence of simultaneous nucleation. Consequently, when the driving force for crystallization increases with increasing EVAL concentration, the initiation of particle nuclei occurs along the entire casting solution simultaneously. Therefore, it is reasonable that uniform particulate membranes were prepared by a homogeneous composition in which a small concentration difference across the membrane can be ignored.

5. Conclusions

Analysis of the solvent evaporation and the phase diagram provides an explanation for the effect of evaporation on membrane morphology. The membrane structure appears to be determined by the state of the evaporated solution when it is immersed in a precipitation bath. Therefore, the evaporation time that is given to the system before the casting solution is immersed into the precipitation bath is important. Macrovoids were found within a membrane when the EVAL solution was immediately immersed into a water bath or with evaporation time less than 15 min. Macrovoids disappear when the evaporation time was 30 min. When the evaporation time was 45 or 60 min, a skinless and symmetric membrane by constituent particles bonded to each other was observed. Two effects can explain solid–liquid demixing which occurs by the longer time of evaporation process. The first one is that the polymer concentration is increased due to the evaporation of solvent. The second cause is that the time available for crystallization is extended to enable solid–liquid demixing to take place. Therefore, solid–liquid demixing can be initiated by small nuclei in the evaporated stage. Subsequently, the membrane formation is completed by liquid–liquid demixing in the immersion stage which particle nuclei have initiated to determine the resulting membrane characteristics.

Acknowledgements

The authors thank the National Science Council of the Republic of China for their financial support of project NSC 86-2216-E-002-003.

References

[1] M. Mulder, Basic Principles of Membrane Technology, Kluwer Academic Publishers, Dordrecht, 1991.
[2] R.E. Kesting, Synthetic Polymeric Membranes, Wiley, New York, 1985.
[3] J.H. Aubert, Isotactic polystyrene phase diagrams and physical gelation, Macromolecules 21 (1988) 3468–3473.
[4] D.R. Lloyd, K.E. Kinzer, H.S. Tseng, Microporous membrane formation via thermally induced phase separation I. Solid–liquid phase separation, J. Membr. Sci. 52 (1990) 239–261.
[5] A.M.W. Bulte, B. Folkers, M.H.V. Mulder, C.A. Smolders, Membranes of semicrystalline aliphatic polyamide nylon 4,6: formation by diffusion-induced phase separation, J. Appl. Polym. Sci. 50 (1993) 13–26.
[6] L.P. Cheng, A.W. Dwan, C.C. Gryte, Membrane formation by isothermal precipitation in polyamide–formic acid–water system I. Description of membrane morphology, J. Polym. Sci. Polym. Phys. 33 (1995) 211–222.
[7] P. van de Witte, H. Esselbrugge, P.J. Dijkstra, J.W.A. van de Berg, J. Feijen, A morphological study of

membranes obtained from the systems polylactide-dioxane-methanol, polylactide-dioxane-water, and polylactide-*N*-methyl pyrrolidone-water, J. Polym. Sci. Polym. Phys. 34 (1996) 2569–2578.
[8] T.H. Young, J.Y. Lai, W.M. Yu, L.P. Cheng, Equilibrium phase behavior of the membrane forming water-DMSO-eval copolymer system, J. Membr. Sci. 128 (1997) 55–65.
[9] L.P. Cheng, T.H. Young, Y.M. You, Formation of crystalline EVAL membranes by controlled mass transfer process in water-DMSO–EVAL copolymer systems, J. Membr. Sci. 145 (1998) 77–90.
[10] T.H. Young, L.W. Chen, L.P. Cheng, Membranes with a microparticulate morphology, Polymer 37 (1996) 1305–1310.
[11] D.T. Lin, L.P. Cheng, Y.J. Kang, L.W. Chen, T.H. Young, Effects of precipitation conditions on the membrane morphology and permeation characteristics, J. Membr. Sci. 140 (1998) 185–194.
[12] L.P. Cheng, H.I. Lin, L.W. Chen, T.H. Young, Solute rejection of EVAL membranes with asymmetric and microparticulate morphologies, Polymer 39 (1998) 2135–2142.
[13] A.J. Reuvers, J.W.A. van der Berg, C.A. Smolders, Formation of membranes by means of immersion precipitation Part I. A model to describe mass transfer during immersion precipitation, J. Membr. Sci. 34 (1987) 45–65.
[14] L.P. Cheng, A.W. Dwan, C.C. Gryte, Membrane formation by isothermal precipitation in polyamide–formic acid–water systems I. Description of membrane morphology, J. Polym. Sci. Polym. Phys. 33 (1995) 211.
[15] L.P. Cheng, A.W. Dwan, C.C. Gryte, Membrane formation by isothermal precipitation in polyamide–formic acid–water systems II. Precipitation dynamics, J. Polym. Sci. Polym. Phys. 33 (1995) 223.
[16] C. Castellari, S. Ottani, Preparation of reverse osmosis membranes. A numerical analysis of asymmetric membrane formation by solvent evaporation from cellulose acetate casting solutions, J. Membr. Sci. 9 (1981) 29–41.
[17] L. Zeman, T. Fraser, Formation of air-cast cellulose acetate membranes Part II. Kinetics of demixing and macrovoid growth, J. Membr. Sci. 87 (1994) 267–279.
[18] S.S. Shojaie, W.B. Krantz, A.R. Greenberg, Dense polymer film and membrane formation via the dry-cast process Part II. Model validation and morphological studies, J. Membr. Sci. 94 (1994) 281–298.
[19] R.Y.M. Huang, X. Feng, Studies on solvent evaporation and polymer precipitation pertinent to the formation of asymmetric polyetherimide membranes, J. Appl. Polym. Sci. 57 (1995) 613–621.
[20] T.H. Young, D.T. Lin, L.Y. Chen, Y.H. Huang, W.Y. Chiu, Membranes with a particulate morphology prepared by a dry–wet process, Polymer 40 (1999) 5257–5264.
[21] W.B. Krantz, R.J. Ray, R.L. Sani, K.J. Gleason, Theoretical study of the transport process occurring during the evaporation step in asymmetric membrane casting, J. Membr. Sci. 29 (1986) 11–36.
[22] C.A. Smolders, A.J. Reuvers, R.M. Boom, I.M. Wienk, Microstructures in phase inversion membranes Part 1. Formation of macrovoids, J. Membr. Sci. 73 (1992) 259–275.
[23] H. Strathmann, K. Kock, P. Pmar, R.W. Baker, The formation mechanism of asymmetric membranes, Desalination 16 (1975) 179–203.
[24] T.H. Young, D.M. Wang, C.C. Hsieh, L.W. Chen, The effect of the second phase inversion on microstructures in phase inversion EVAL membranes, J. Membr. Sci. 146 (1998) 169–178.